Supplementary Information (SI) for Nanoscale.

Supplementary materials

On-receptor computing with classical associative learning in semiconductor oxide memristors

Dongyeol Ju,[a] Jungwoo Lee,[a] Sungjun Kim[a]

[a] Division of Electronics and Electrical Engineering, Dongguk University, Seoul 04620, South Korea

E-mail: sungjun@dongguk.edu

Table. S1 The comparison of Pt/IGZO/SnO_x/TiN device's nociceptive and synaptic behavior compared to previous works.

No	Structure	Nociceptive function	Synaptic function	Multifunctional behavior	Reference
1	Pt/SiO_x:Ag/Ag/Pt	Threshold, no-adaptation, relaxation, sensitization	X	X	[S1]
2	Pt/HfO_2/TiN	Threshold, relaxation, sensitization	X	X	[S2]
3	CZO/ITO/glass	Threshold, no-adaptation, relaxation, sensitization, recovery	Potentiation and depression	X	[S3]
4	Ag/SiC/Pt	Threshold, no-adaptation, relaxation	STDP	X	[S4]
5	s-ITO/c-ITO	Threshold, no-adaptation, relaxation, sensitization	X	X	[S5]
6	ITO/TiO_x/TiN	Threshold, no-adaptation, relaxation, sensitization	X	X	[S6]
7	Au/MoS_2/Ag	Threshold, no-adaptation, relaxation, sensitization	X	X	[S7]
8	Au/$CsPbBr_3$/ITO	X	Potentiation and depression, PPF, STM and LTM	X	[S8]
9	Ti/TaO_x/ITO	X	Potentiation and depression, STDP	X	[S9]
10	Ag/TiO_2/Pt	Threshold, no-adaptation, relaxation, sensitization	STM and LTM, SRDP, STDP	X	[S10]
11	Pt/IGZO/SnO_x/TiN	Threshold, no-adaptation, relaxation, sensitization, recovery	Learning and forgetting, STM and LTM, SRDP	Pavlovian conditioning, reservoir computing	This work

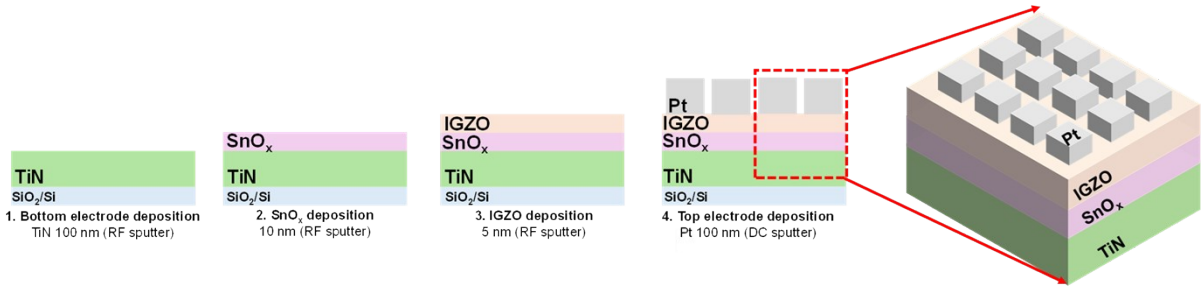

Fig. S1 Fabrication process of the Pt/IGZO/SnO_x/TiN memristor.

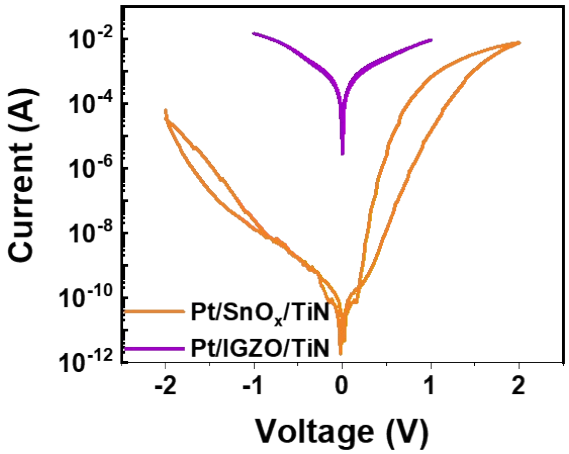

Fig. S2 The I-V curves of Pt/SnO_x/TiN and Pt/IGZO/TiN devices.

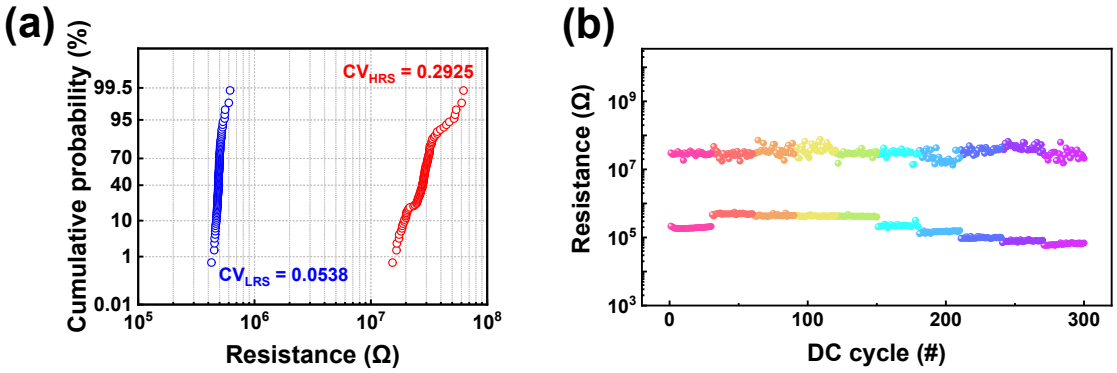

Fig. S3 (a) Coefficient of variation of 100 DC endurance cycles of the Pt/IGZO/SnO_x/TiN memristor. (b) Uniformity of endurance properties over 10 different randomly selected Pt/IGZO/SnO_x/TiN devices, each showcasing 30 cycles.

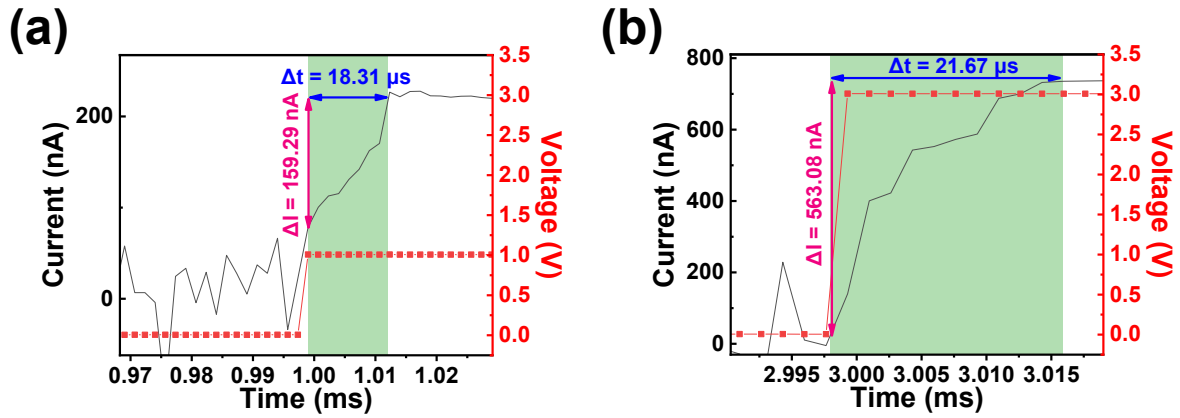

Fig. S4 Energy consumption of the Pt/IGZO/SnO_x/TiN device. (a) Energy consumption of read process, resulting 2.92 pJ. (b) Energy consumption of write process, resulting 36.6 pJ.

Table. S2 The key parameter comparison of Pt/IGZO/SnO_x/TiN device compared to previous works.

No	Structure	Switching film thickness	Endurance	Operating current	Power consumption	Switching type	Memory storing function	Reference
1	ITO/MoS_2/EGaIn	25 nm-	> 10^3	< 0.1 A	32.9 pJ	Digital	Non-volatile	[S11]
2	VO_x/SiO_2/Si	140 / 2.1 nm	N/A	N/A	0.53 pJ	Digital	Non-volatile	[S12]
3	Au/MoS_2/Au	N/A	> 400	< 1 mA	200 pJ	Digital	Non-volatile	[S13]
4	Pt/ZrO_2/IGZO/TiN	3 / 5 nm	> 100	< 4 mA	4 μJ	Digital	Non-volatile	[S14]
5	Ag/SiC/Pt	10 nm	> 100	< 10 μA	32.25 pJ	Digital	Non-volatile	[S4]
6	Ag/MoS_2/Pt	30 nm	> 10^6	N/A	400 nJ	Digital	Non-volatile	[S15]
7	Ag/$Ti_3C_2T_x$ NS/Pt	N/A	N/A	< 50 μA	18.82 nJ	Digital	Volatile	[S16]

8	TiN/SiO$_2$/TaO$_x$/Pt	25 / 2 nm	N/A	< 1 mA	N/A	Digital	Non-volatile	[S17]
9	Ti/TaO$_x$/ITO	10 nm	> 10^3	< 10 mA	N/A	Digital	Non-volatile	[S9]
10	Pt/IGZO/SnO$_x$/TiN	10 / 5 nm	> 100	< 500 μA	36.6 pJ	Analog	Volatile	This work

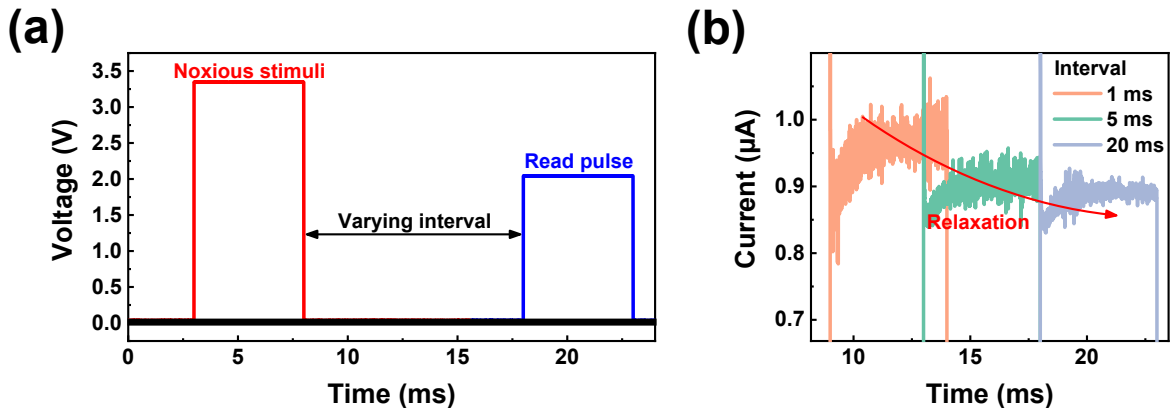

Fig. S5 (a) Pulse schematic utilized to gain the relaxation properties of the Pt/IGZO/SnO$_x$/TiN device. (b) Current response at different relaxation periods.

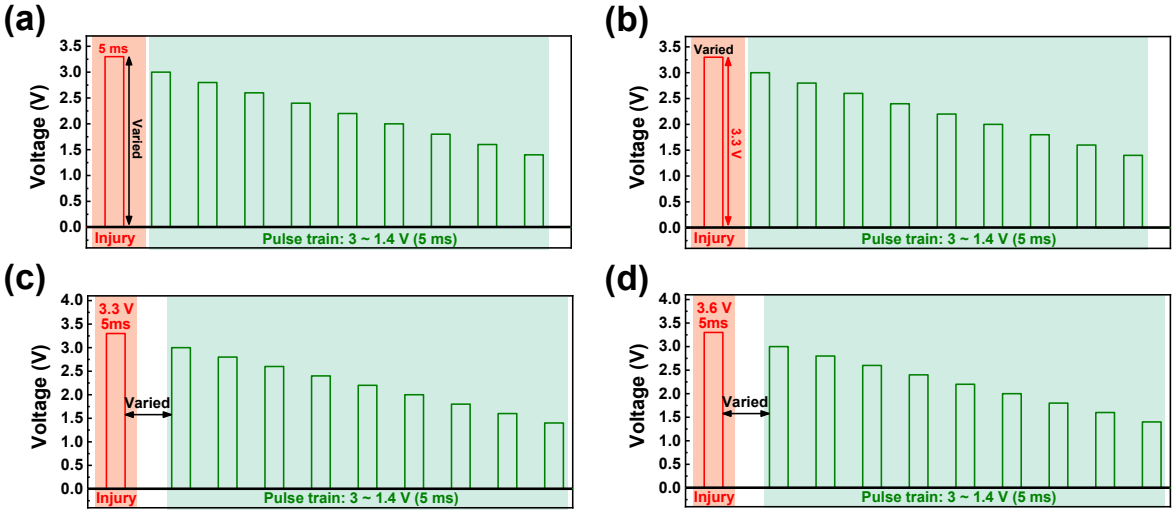

Fig. S6 Pulse schematic utilized to gain sensitization properties of the Pt/IGZO/SnO_x/TiN device, earned through differing (a) injury amplitude, and (b) injury width. Pulse schematic utilized to observe recovery under injury of (c) 3.3 V, and (d) 3.6 V.

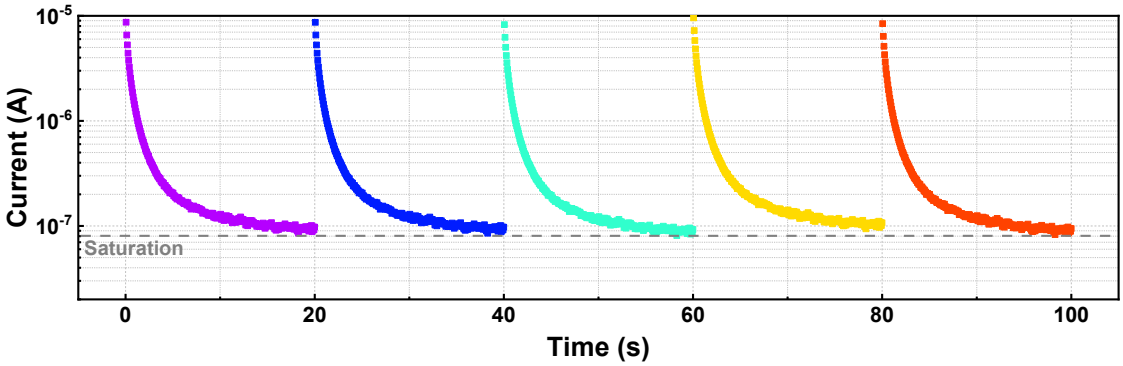

Fig. S7 Repeated LTM transition behavior under application of 50 set pulses.

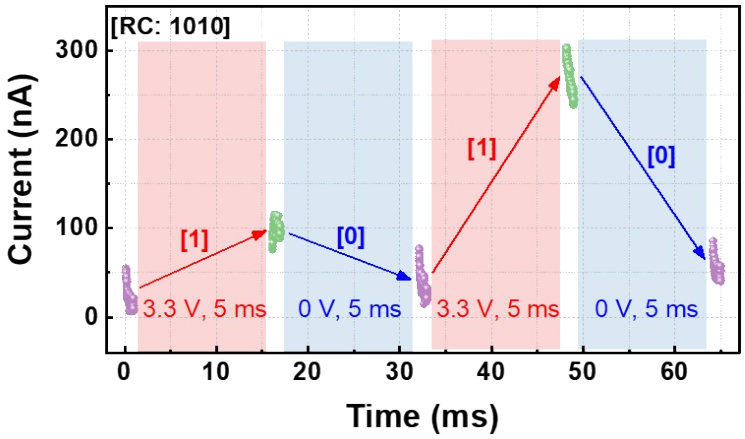

Fig. S8 Schematic illustration of current response of 4-bit reservoir computing following the use of a [1010] pulse.

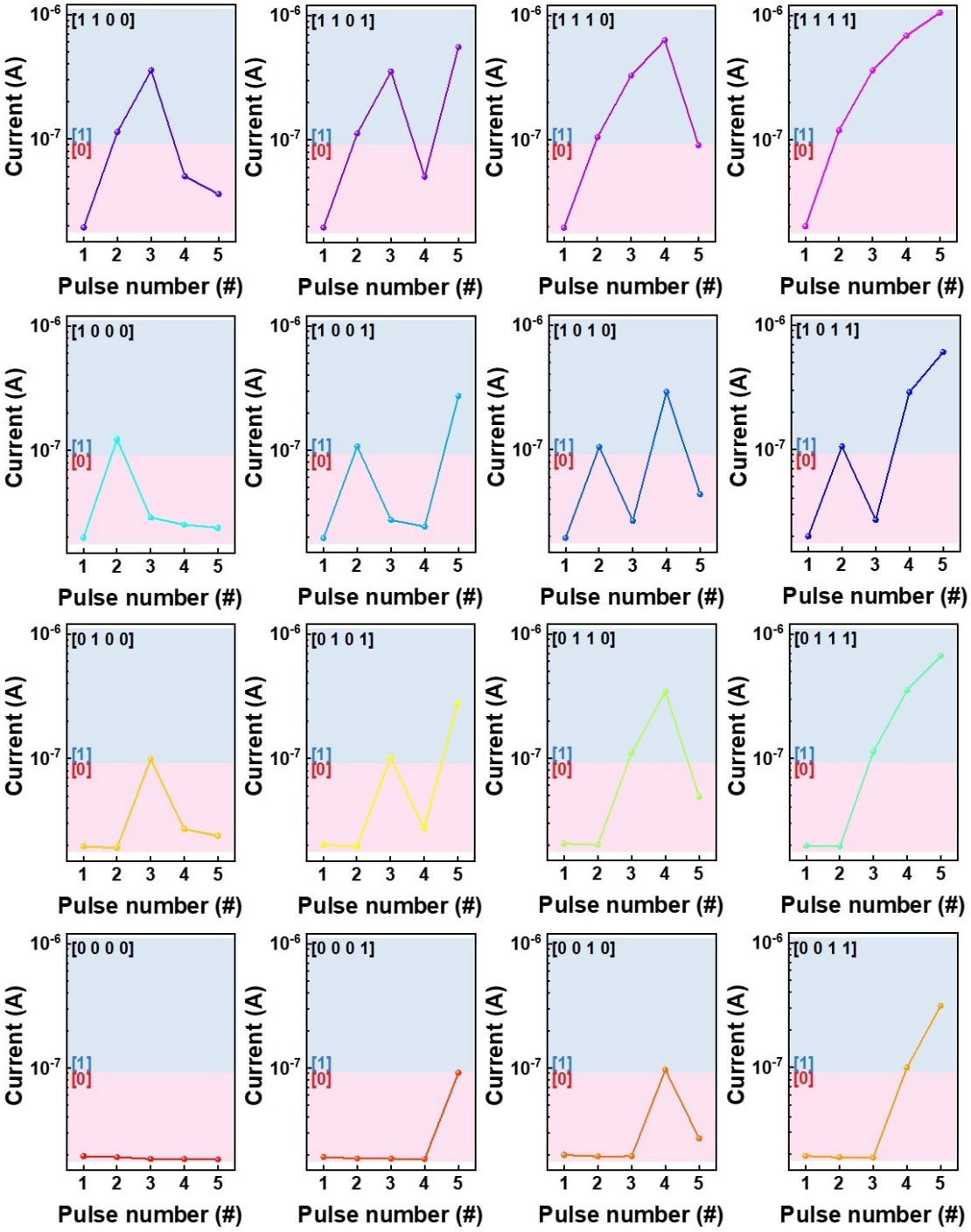

Fig. S9 Sixteen different reservoir states of the 4-bit reservoir computing based on Pt/IGZO/SnO_x/TiN device.

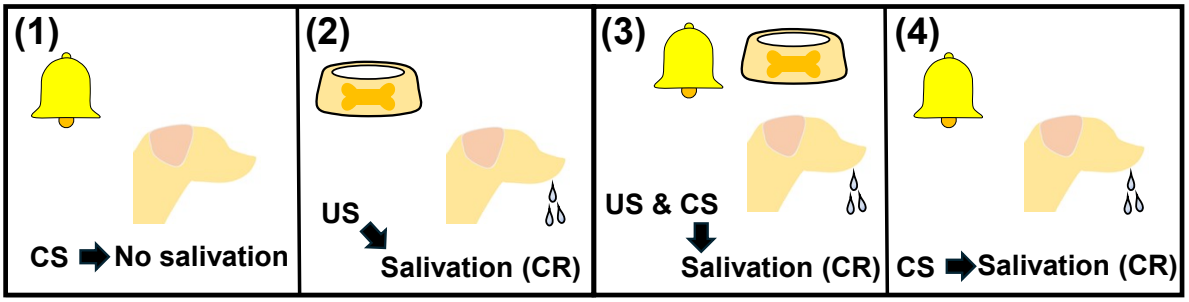

Fig. S10 Schematic illustration of Pavlovian conditioning process.

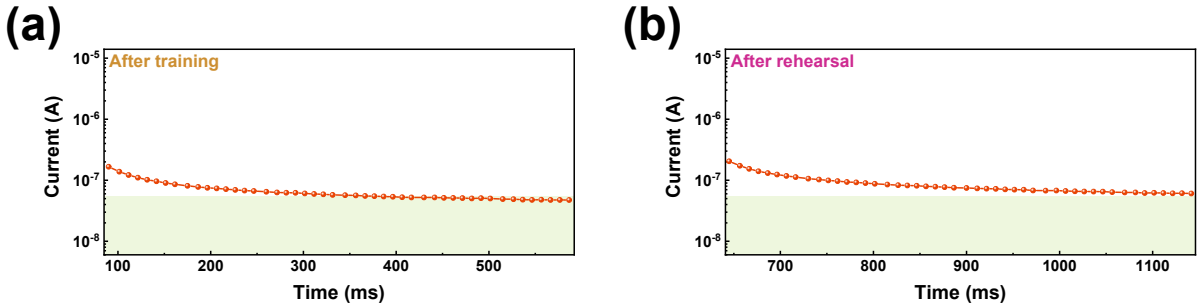

Fig. S11 Facilitation of current observed from Pavlovian conditioning for 500 s after (a) training, and (b) rehearsal.

References

[S1] J. H. Yoon, Z. Wang, K. M. Kim, H. Wu, V. Ravichandran, Q. Xia, C. S. Hwang and J. J. Yang, Nat. Commun., 2018, 9, 417.

[S2] Y. Kim, Y. J. Kwon, D. E. Kwon, K. J. Yoon, J. H. Yoon, S. Yoo, H. J. Kim, T. H. Park, J. W. Han, K. M. Kim and C. S. Hwang, Adv. Mater., 2018, 30, 1704320.

[S3] R. Mandal, A. Mandal and T. Som, Appl. Mater. Today, 2024, 37, 102103.

[S4] L. Liu, J. Zhao, G. Cao, S. Zheng and X. Yan, Adv. Mater. Technol., 2021, 6, 2100373.

[S5] X. Han, Y. Xu, B. Sun, R. Xu, J. Xu, W. Hong, Z. Fu, H. Zhu, X. Sun, J. Chang and K. Qian, Appl. Phys. Lett., 2022, 120, 094103.

[S6] Y. Zhang, F. Wang, X. Shan, X. Lin, X. Zhao, Q. Zhou, K. Shan, Z. Ma, G. Chen, X. Wang, D. Huang and K. Zhang, Mater. Sci. Eng. B-Adv. Funct. Solid-State Mater., 2023, 290, 116360.

[S7] D. Dev, M. S. Shawkat, A. Krishnaprasad, Y. Jung and T. Roy, IEEE Electron Device Lett., 2020, 41, 1440–1443.

[S8] F. Luo, W. M. Zhong, X. G. Tang, J. Y. Chen, Y. P. Jiang and Q. X. Liu, Nano Mater. Sci., 2024, 6, 68-76.

[S9] D. Ju, J. H. Kim and S. Kim, J. Alloys Compd., 2023, 961, 170920.

[S10] M. C. Sahu, A. K. Jena, S. K. Mallik, S. Roy, S. Sahoo, R. S. Ajimsha, P. Misra and S. Sahoo, ACS Appl. Mater. Interfaces, 2023, 15, 25713–25725.

[S11] P. Saha, M. Sahad E, S. Sathyanarayana and B. C. Das, *ACS Nano*, 2024, 18, 1137-1148.

[S12] M. Kumar, J. Y. Park and H. Seo, *Small Methods*, 2021, 5, 2100566.

[S13] E. Lee, J. Kim, J. Park, J. Hwang, H. Jang, K. Cho and W. Choi, *ACS Appl. Mater. Interfaces*, 2023, 15, 15839-15847.

[S14] X. Chen, Y. Jin, Z. Tao, L. Jiang, X. Wu, Y. Xiao, B. Jiang, X. Wen, J. Zhang, M. Zhu and C. Ye, *IEEE Trans. Electron Devices*, 2023, **70**, 1001–1005.

[S15] K. Wang, L. Li, R. Zhao, J. Zhao, Z. Zhou, J. Wang, H. Wang, B. Tang, C. Lu, J. Lou, J. Chen and X. Yan, *Adv. Electron. Mater.*, 2020, 6, 1901342.

[S16] A. Sokolov, M. Ali, H. Li, Y. R. Jeon, M. J. Ko and C. Choi, *Adv. Electron. Mater.*, 2021, 7, 2000866.

[S17] Z. Wang, M. Yin, T. Zhang, Y. Cai, Y. Wang, Y. Yang and R. Huang, *Nanoscale*, 2016, **8**, 14015–14022.